

# Comparative study of localized side group in poly(2,3 and 4 methyl cyclohexyl methacrylate)s. TSDC measurements

Gustavo Domínguez-Espinosa<sup>a</sup>, Maria J. Sanchis<sup>a</sup>, Ricardo Díaz-Calleja<sup>a,\*</sup>,  
Claudia Pagueguy<sup>b</sup>, Ligia Gargallo<sup>b</sup>, Deodato Radic<sup>b</sup>

<sup>a</sup> *Departamento de Termodinámica Aplicada, E.T.S.I.I., Universidad Politécnica de Valencia, Camino de Vera s/n, 46071 Valencia, Spain*

<sup>b</sup> *Departamento de Química Física, Facultad de Química, Pontificia Universidad Católica de Chile, Casilla 306, Santiago 22, Chile*

Received 1 March 2005; received in revised form 29 July 2005; accepted 4 October 2005

Available online 21 October 2005

## Abstract

By means of thermal sampling techniques, the fine structure of the  $\gamma$ -relaxation zone of poly(methyl cyclohexyl methacrylate)s (P2MCHMA), (P3MCHMA), (P4MCHMA) were analyzed. Results reveal that in this relaxation zone, at least two peaks are present. These peaks are attributed to the cis and trans isomers. Loss permittivity of the polymers under study in this relaxation zone has been reproduced from the partial depolarization data by using the elementary relaxation times and activation energies. Results are in relatively good agreement with the experimental data previously obtained. Molecular mechanic calculations have been carried out in order to elucidate the characteristics and molecular origin of the relaxations observed in this zone. An interpretation of the height of the peaks associated to the cis- and trans-isomer in terms of strain energy (SE) have been carried out.

© 2005 Elsevier Ltd. All rights reserved.

**Keywords:** Poly(methyl cyclohexyl methacrylate)s; Thermally stimulated depolarization currents; Molecular mechanics calculations

## 1. Introduction

It is well known [1–4] that the mechanical  $\gamma$  process, which is observed about 193 K (1 Hz) in polymers with cyclohexyl groups, is associated to the chair-to-chair conformational transition in this ring [4]. On the other hand, in acrylic polymers, the presence of bulky side groups tend to inhibit the motions of the side chain [3], depressing the intensity of the relaxations. Dielectric data [5] also indicates the presence of significant dielectric activity in the same temperature zone. In order to gain a better understanding on the nanoscale mechanisms underlying subglass relaxations, it is advisable to investigate the relaxational behaviour of polymers having side groups with slightly different structures. In fact, experimental results indicate that the position and intensity of the  $\gamma$  peaks are influenced not only by the environment and the chemical nature of the moieties linking the rings to the main chain but also by substituents of the hydrogen atoms of the rings [6]. For this reason, methyl substitution in the three possible positions

in the ring should give significant differences in their corresponding dielectric activity.

Molecular motions giving rise to relaxation processes which involves the overcoming of energy barriers whose activation parameters are significantly associated to each relaxation process. For this reason, molecular mechanic studies on specific molecular motions of polymers have been revealed as a very useful tool in order to predict the energies associated with each conformational change in the molecule. However, molecular mechanic energies are not absolute quantities and only differences in energies between two conformations are meaningful. In the present case, the chair-to-chair interconversion is a complicated process produced by successive conformational changes within the molecule and for this reason a detailed study of this particular motion is advisable.

## 2. Experimental section

### 2.1. Monomer and polymer preparation

Methacrylates were obtained by reaction of methacryloyl chloride with the corresponding alcohols (50/50% cis–trans conformations) in toluene using triethylamine as acid acceptor, following a procedure previously reported [7,8]. Monomers were polymerized under vacuum, in toluene solutions at 323 K

\* Corresponding author.

E-mail address: [rdiazc@ter.upv.es](mailto:rdiazc@ter.upv.es) (R. Díaz-Calleja).

using  $\alpha,\alpha'$ -azo-bisobutyronitrile as initiator. Polymers were purified by successive reprecipitations with methanol. Samples were vacuum dried at 303 K during several days. The calorimetric glass transition temperature ( $T_g$ ), measured at 20 K min<sup>-1</sup> in DSC-Q10 from TA Instruments, were 371, 374 and 394 K, for P2MCHMA, P3MCHMA and P4MCHMA, respectively.

## 2.2. Thermally stimulated depolarization current experiments (TSDC)

TSDC experiments [9] were carried out with a TSC-RMA (Thermold 9000) spectrometer on polymer pills of 1 mm of thickness and 76 mm<sup>2</sup> of surface. The global spectrum was obtained by poling the sample at 403 K for P2MCHMA and P3MCHMA and 358 K for P4MCHMA under a electric field of 300 V mm<sup>-1</sup>, after quenching at 113 K. Then the field was removed, the electrodes short circuited, and was warmed at the constant rate of 7 K min<sup>-1</sup>. From the time derivative of the depolarization ( $J = -dP/dt$ ), the global spectrum was obtained. Partial polarization discharge current experiments were also performed by using poling windows of 5 K. In all cases, the limits of the depolarization curves were 15 K below and 40 K above the polarization temperatures  $T_p$ .

## 2.3. Simulation methodology and computational details

Molecular mechanics calculations were performed using the force field method developed by Allinger and co-workers [10–12]. The PC-MODEL software [13] was employed to carry out the calculations. It is based on an empirical force field, called MMX that is derived from MM2(P) [14].

This empirical force field includes intermolecular as well as intramolecular contributions. The non-bonded energy function expresses interactions between atoms, which are not bonded to each other. It is splitted into a van der Waals steric component and electrostatic component, dealing with interactions between charges and dipoles. A Buckingham potential was used for this purposes. Parametrization of MMX has been carried out, assuming an artificial dielectric constant of 1.5.

The intramolecular energy function is splitted into a connectivity term, the bond stretching function and flexibility terms, the angle bending and the torsional functions, as well as cross-terms describing the coupling of stretch–bend, bend–bend and torsional–stretch interactions are take into account. The Wilson ( $E_{OOP}$ , our umbrella out-of-plane) term has been also included, but their contribution to the global energy was small in all cases.

The first step in the calculations is to establish an initial geometry. Exploration of the conformational characteristics of representative skeletal fragments of the polymers is therefore a prerequisite to adequately model larger fragments. The calculations of the theoretical energy requirements for a bond rotation were carried out with models compounds of one unit for each polymer, which simulate part of the polymer chain. The minimization was performed using a combination of steepest descent and Newton–Raphson methods [15] till

the energy gradient falls below 0.0004 kJ mol<sup>-1</sup> Å<sup>-1</sup> for each specific conformer.

## 3. Results and discussion

### 3.1. Thermally stimulated depolarization current experiments (TSDC)

In order to analyze as a whole the relaxation processes in these materials, thermostimulated depolarization currents (TSDC) experiments, were carried out. The global TSDC spectra for the polymers under study are represented in Fig. 1. The thermograms vaguely remind the experimental Ac isochrones at low frequency reported at a previous study by dielectric relaxation spectroscopy [16].

The global TSDC curves in the glassy region show prominent  $\gamma$  peaks whose maxima are roughly located at ~165 K (P2MCHM), ~155 K (P3MCHM) and ~148 K (P4MCHM). These  $\gamma$  peaks show structure, and therefore two relaxation processes mutually overlapping are assumed. These two processes can be associated to the existence of an approximate equimolar mixture of cis–trans conformational isomers in the original alcohols, which are the responsible to obtain polymers containing a mixture of both isomers. This result is in contrast with Ac conventional dielectric measurements, where such splitting is not observed due to the relatively high frequency of the experiments. It is known that at lower frequencies a better resolution of the peaks is observed. For this reasons TSDC technique is particularly useful. In this way, the splitting of the two  $\gamma$  peaks (cis- and trans-isomers) on TSDC curves was observed. For this reason is advisable to carry out a more detailed study of the  $\gamma$  relaxation zone.

Increasing the temperature prominent  $\alpha$  peaks, associated to the dynamic glass transition are also observed at ~345 K (P2MCHMA), ~350 K (P3MCHMA) and ~370 K (P4MCHMA).

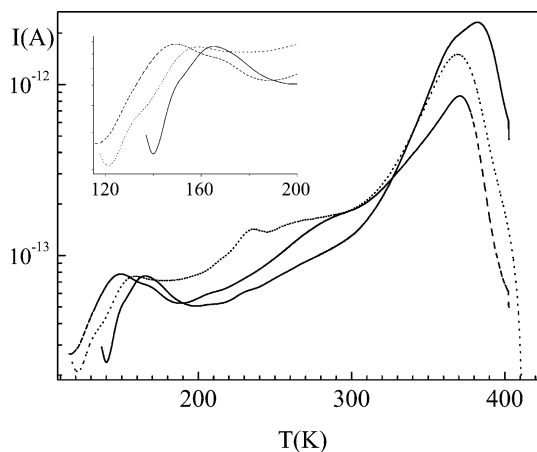


Fig. 1. Global TSDC spectrum of (—) P2MCHMA, (···) P3MCHMA and (---) P4MCHMA, over the glassy and glass-rubber regions. Inset: details of the curves in the glassy state.

Moreover, between  $\alpha$  and  $\gamma$  peaks poorly defined  $\beta$  peaks in the range from 230 to 280 K are also observed.

The TSDC peak, can be obtained from the current density  $J(T)$  measured during a TSDC experiment.  $J(T)$  is given by [17]

$$J(T) = \frac{P_e(T_p)}{\tau_0} \exp\left(-\frac{E_a}{kT}\right) \exp\left[\frac{-1}{h\tau_0} \int_{T_0}^T \exp\left(-\frac{E_a}{kT'}\right) dT'\right] \quad (1)$$

where  $P_e(T_p)$  is the equilibrium or steady-state polarization at the polarizing temperature  $T_p$ ,  $k$  is the Boltzmann's constant and  $h$  is the heating rate, which is constant in the experimental conditions used. In this equation an Arrhenius dependence of the relaxation times on temperature was postulated. When TSDC reaches the maximum temperature  $T_{\max}$  of the peak,  $(dJ/dT)_{T=T_{\max}}$  leads to zero. The equivalent frequency  $f_{\text{eq}}$  at the maxima of the peaks can be obtained by differentiating Eq. (1),

$$f_{\text{eq}} = \frac{hE_a}{2\pi kT_{\max}^2} \quad (2)$$

According to this equation, and taking into account the activation energies values,  $E_{a\gamma}$ , previously calculated [16], the calculated value for  $f_{\text{eq}}$  corresponding to the  $\gamma$  peaks are approximately the same for all the polymers under study, and close to  $4 \times 10^{-3}$  Hz. This frequency is lower than that used in dielectric spectroscopy, but its value can be useful in order to correlate both types of measurements. In fact, extrapolations of the Arrhenius type plots corresponding to the  $\gamma$ -relaxation, obtained from dielectric relaxation spectroscopy (DRS) experiments [16], are in good agreement with the frequencies given by Eq. (2), as we can observe in Fig. 2.

Thermal windowing TSDC experiments were carried out in order to reveal the details of the  $\gamma$  processes observed in the global spectra. These experiments make it possible to activate the narrow fractions or segments of the global peak, and to decompose the broad relaxation spectrum into its elementary components by assuming a single relaxation time for each peak. Experiments were performed in the glassy state using

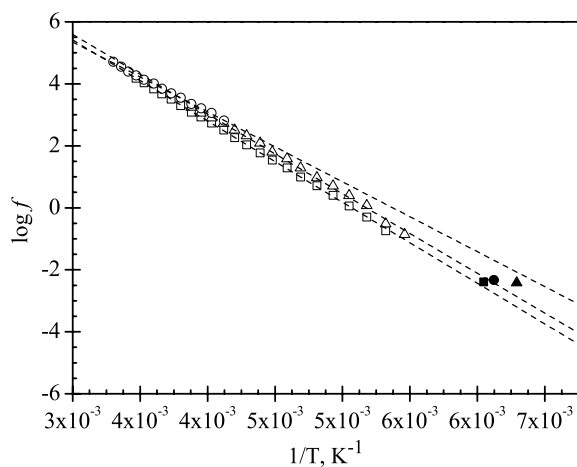


Fig. 2. Dependence of  $\ln f$  versus inverse of temperature in  $\gamma$  zone for (■) P2MCHMA, (●) P3MCHMA and (▲) P4MCHMA (open symbols by DRS and filled symbols by TSDC).

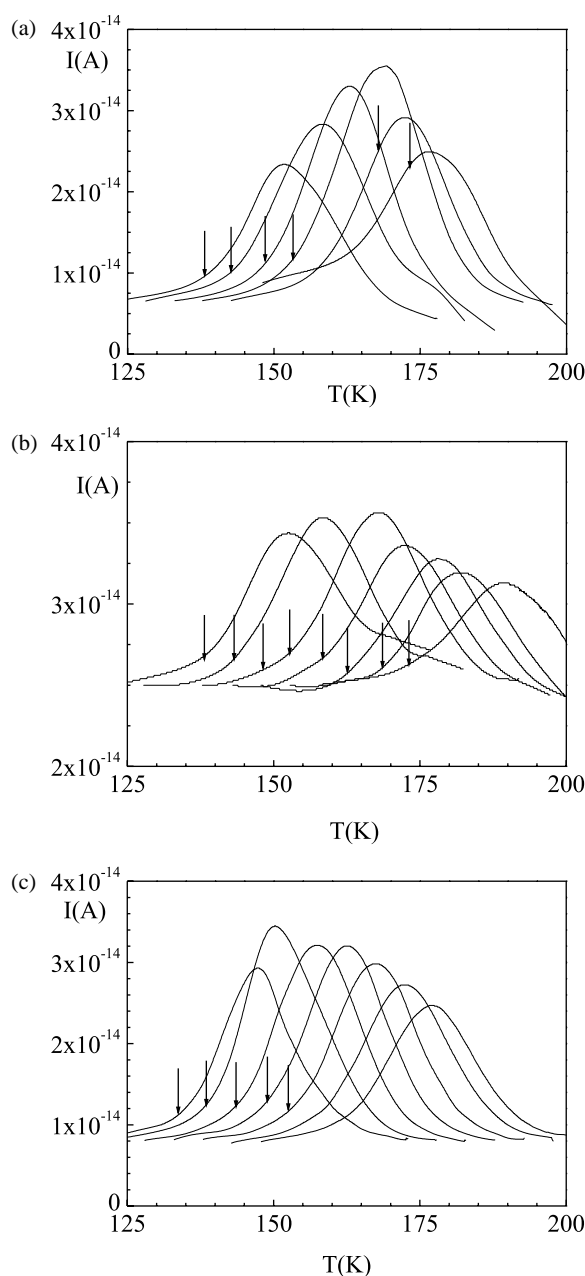


Fig. 3. Elementary subglass ( $\gamma$  peak) TSDC spectra obtained at the following poling temperatures  $T_p$  (K): (a) P2MCHMA (138, 143, 148, 153, 168, 173); (b) P3MCHMA (138, 143, 148, 153, 158, 163, 168) and (c) P4MCHMA (133, 138, 143, 148, 153). Arrows indicate the polarization temperature ( $T_p$ ) in each case.

poling temperatures  $T_p$  lying in the range 133–213 K. The elementary relaxation processes thus obtained, shown in Fig. 3, present a peak whose maxima intensity corresponds at one temperature ( $T_{\max}$ ) that are a linear function of  $T_p$ . In the range of  $\gamma_i$  processes, the TSDC thermal windowing experiments show that the elementary peaks are rather symmetrical and the shapes of the peaks do not change noticeably in this temperature range. In order to calculate the activation parameters, from the curves obtained in windowing experiments, it has been assumed that every elementary cleaning curve can be described by a single relaxation time, whose

temperature dependence is given by [18]

$$\tau(T) = \frac{\int_{T_0}^T J(T)dT}{hJ(T)} \quad (3)$$

where  $h$  is the constant heating rate and  $T_0$  is the extreme temperature at the lower side of each peak.

Eq. (3) shows that integration of the elementary TSDC windowing curves allows us to obtain the temperature dependence of the relaxation time. The temperature evolution of the relaxation times is expressed by the Arrhenius equation

$$\tau(T) = \tau(T_0)\exp\left(\frac{E_a}{kT}\right) \quad (4)$$

where  $\tau_0$  is a pre-exponential factor and  $E_a$  is the activation energy for the process. The plot of  $\log \tau$  against  $1/T$  is linear, at least up to the half width temperature. By this way the pre-exponential factor and the activation energy can be obtained from the linear part of the curves. The values of  $\tau_0$  and  $E_a$  are summarized in Table 1. It can be seen in this table that the values of the activation energy seem to increase and the values of the pre-exponential factor seem to decrease, with  $T_p$ . Nevertheless, according to the theory of TSDC [17],  $\tau_0$  is a decreasing function of  $T_p$ . Moreover, the results show that the  $E_a$  is distributed in the ranges  $\sim 27$ – $58$  kJ mol<sup>-1</sup> in relatively good agreement with the obtained values from dielectric relaxation spectroscopy [16]. The  $\tau_0$  values change with temperature from  $10^{-8.4}$  to  $10^{-11}$  s, and these values are typical of the local relaxation processes.

The relaxation strength of each elementary peak was calculated by means of the expression [19,20]

$$\Delta\varepsilon = \varepsilon_0 - \varepsilon_\infty = \frac{\int_{T_0}^T J(T)dT}{\varepsilon_{\text{vac}}hAE} \quad (5)$$

where  $\varepsilon_\infty$  and  $\varepsilon_0$  represent, respectively, the relaxed and unrelaxed dielectric relative permittivity for each peak,  $\varepsilon_{\text{vac}}$  is the dielectric permittivity in vacuum,  $A$  is the area of the sample,  $E$  is the electric field, and  $T_0$  and  $T_\infty$  are, the extreme temperatures at the low and high temperature side of the peaks, respectively. The values of the calculated relaxation strength for the elementary peaks, plotted as a function of  $T_p$ , give a curve whose shape reminds one of that of the global TSDC spectrum in the glassy region (Fig. 1).

It is interesting to analyze the components of the complex dielectric permittivity at very low frequencies as obtained from the thermal sampling analysis. For this purpose, the values of  $\varepsilon'$

and  $\varepsilon''$  obtained from the elementary TSDC peaks for the three polymers under study have been calculated according to the following expressions [21,22]

$$\varepsilon' = \varepsilon_\infty + \sum_{i=1}^n \frac{\Delta\varepsilon_i}{1 + \omega^2\tau_i^2(T)}; \quad \varepsilon'' = \sum_{i=1}^n \frac{\Delta\varepsilon_i\omega\tau_i(T)}{1 + \omega^2\tau_i^2(T)} \quad (6)$$

where  $\Delta\varepsilon_i$  is the relaxation strength,  $\varepsilon_\infty$  the relaxed dielectric constant,  $\omega$  is the angular frequency and  $\tau_i(T)$  is the Debye relaxation time for the system  $i$  in which its temperature dependence is determined by Eq. (4). The number  $n$  in the sum of Eq. (6) denotes numbers of a series of elementary spectra isolated by TSDC experiments (Fig. 3). Activation energies ( $E_{ai}$ ) and pre-exponential factors ( $\tau_{0i}$ ), corresponding to the  $i$ th elementary spectra used in the calculations is shown in Table 1. In order to obtain a good agreement between the calculated and the experimental permittivities, it is advisable to choose the more adequate range of temperatures in such a way that only one relaxation process were covered, thus avoiding overlapping with the next relaxation peak.

The temperature dependences of the loss permittivity obtained from Eq. (6) at  $10^{-4}$  Hz, for the three polymers under study, are shown in Fig. 4. The isochrone presents a complex pattern, showing at least two relaxation processes. We interpret these relaxations in terms of the two isomers existing in the cyclohexanol used to prepare the monomers and polymers. In any case the position of the dominant peaks for all polymers agrees well with the extrapolated Arrhenius plot of Fig. 2 observed in DRS experiments. In the same way the height of the peaks are also in good agreement with the experimental dielectric data at higher frequencies [16] (see inset Fig. 4).

To characterize and to analyze loss permittivity spectra in a more detailed way the observed relaxations, it is convenient to split the observed peaks in their components. For this purpose,

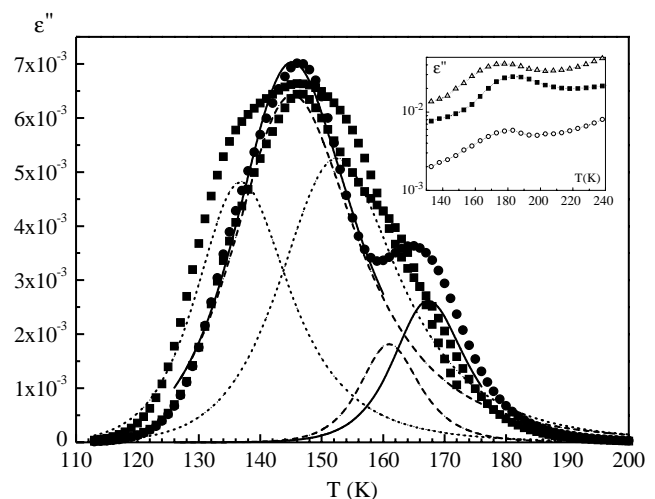


Fig. 4. Loss factor simulation data (symbols) and their deconvolution in two FK function (lines) as function of temperature, at  $10^{-4}$  Hz for P2MCHMA (■—), P3MCHMA (●, - - -) P4MCHMA (▲, ···), showing the two  $\gamma$  peaks. The low and high temperature peaks correspond, respectively, to the trans- and cis-isomers, for P2MCHMA and P4MCHMA. For P3MCHMA, the inverse order is present. Inset: DRS spectra at  $10^{-1}$  Hz for three polymers.

Table 1  
Activation energies (kJ mol<sup>-1</sup>) calculated from Arrhenius plot

| Polymer | $\gamma$ (trans) | $\gamma$ (cis)   |
|---------|------------------|------------------|
| P2MCHMA | $38.44 \pm 0.06$ | $47.61 \pm 0.15$ |
| P3MCHMA | $43.77 \pm 0.67$ | $38.98 \pm 0.47$ |
| P4MCHMA | $40.34 \pm 0.24$ | $43.43 \pm 0.37$ |

a model must be chosen to appropriately reproduce the experimental data. A reliable model to represent the secondary relaxations in polymers is the symmetric Fuoss and Kirkwood equation (FK) [23]. If, according to our hypothesis, it is assumed that the  $\gamma$  process is the result of two overlapping processes, then the loss permittivity curves can be fitted to the addition of two Fuoss–Kirkwood equations according to the following scheme

$$\varepsilon'' = \sum_{i=1}^2 \varepsilon''_{\max}^{(i)} \operatorname{sech} \frac{m^{(i)} E_a^{(i)}}{R} \left( \frac{1}{T} - \frac{1}{T_{\max}^{(i)}} \right) \quad (7)$$

where  $R$  is the gas constant and for each process  $i$ ,  $E_a^{(i)}$  are the activation energy,  $T_{\max}^{(i)}$  the temperature of the maximum, and  $m^{(i)}$  a shape parameter ( $0 < m < 1$ ) related to the broadness of the relaxation in the sense that the lower  $m$ , the wider the distribution is. The value of  $m=1$  corresponds to a single relaxation time (Debye peak). The function was determined from the multiple non-linear regression analysis of the experimental data, allowing the variation of the three characterizing peak parameters ( $\varepsilon''_{\max}^{(i)}$ ,  $(m^{(i)} E_a^{(i)})/R$ ,  $T_{\max}^{(i)}$ ). Using the  $T_{\max}^{(i)}$  temperature of the maximum for each frequency obtained in the fitting procedure, the activation energy values were obtained by the Arrhenius plot for each one of the two  $\gamma$  processes obtained for three polymers under study (Fig. 5).

In the analysis of the viscoelastic relaxations on this type of polymers, Heijboer [1] has concluded that the poly(*trans*-4-cyclohexyl methyl methacrylate) and poly(*cis*-4-cyclohexyl methyl methacrylate) show  $\gamma$  peaks at different temperatures for each polymer, and the position of the methyl substituent in the ring has a marked influence on the height of the maxima.

Our results also show differences, in the position and the height of the maxima of the peaks, corresponding to the *cis*- and *trans*-conformers in each polymer. Accordingly, the assignation for each polymer, of the low temperature process to the *trans*-isomer and the high temperature process to *cis*-isomer has been made for P2MCHMA and P4MCHMA. In the case of

P3MCHMA the inverse situation is present. The height of the maxima,  $\varepsilon''_{\max}^{(i)}$  obtained in the fitting procedure at the frequency of  $10^{-4}$  Hz show, that  $\varepsilon''_{\max}^{(i)}(\text{cis-P4MCHMA}) \approx 1.7 \varepsilon''_{\max}^{(i)}(\text{trans-P4MCHMA})$  in good agreement with Heijboer's results [1]. The same tendency is observed for the P3MCHMA,  $\varepsilon''_{\max}^{(i)}(\text{cis-P3MCHMA}) \approx 3.4 \varepsilon''_{\max}^{(i)}(\text{trans-P3MCHMA})$ . On the contrary, the relation between the height of the  $\gamma$  peaks for the P2MCHMA were  $\varepsilon''_{\max}^{(i)}(\text{trans-P2MCHMA}) \approx 2.7 \varepsilon''_{\max}^{(i)}(\text{cis-P2MCHMA})$ .

In Table 1 the activation energies corresponding to the two  $\gamma$ -relaxations calculated from Arrhenius plots are summarized. Thus, the activation energies range between 38 and 48 kJ mol<sup>-1</sup>, the higher and lower values corresponding to P2MCHMA.

### 3.2. Molecular mechanics study of $\gamma$ -relaxation

In order to elucidate the specific motions responsible of the observed secondary  $\gamma$ -relaxations, we studied the specific role of each part of the molecule in the three polymers under study and the PCHMA polymer. To start with, we assume, in agreement with Heijboer [1], that the observed relaxation is mainly due to the barrier preventing the chair-to-chair interconversion of the cyclohexyl group. The chair-to-chair interconversion is a complicated process produced by successive conformational changes within the molecule and is best visualized with the aid of molecular models. For this reason, molecular simulation techniques are a strong tool in order to provide an explanation of the molecular origin of the observed secondary  $\gamma$ -relaxations.

There are two types of carbon–hydrogen bond positions in the chair conformation of cyclohexyl group. Six bonds are parallel to a vertical axis (axial bonds) and six lie in a region corresponding to the approximate ‘equator’ of the molecule (equatorial bonds). The shortest distances between non-bonded atoms are those involving axial hydrogen's on the same side of the molecule. A rapid process of chair-to-chair transition becomes the six axial and six equatorial hydrogen atoms in cyclohexyl group. Moreover, when a hydrogen atom is substituted by a methyl group, two geometric isomers are possible (*cis*–*trans* isomers). The methyl group can be either *cis* or *trans* with respect to the bond that links the cyclohexyl ring to the chain.

When an isolated cyclohexyl ring undergoes internal rotations, the result is a conformational change in the ring. It is well known that the chair-to-chair transition in the cyclohexyl ring follows the sequence given by chair  $\rightarrow$  half-chair  $\rightarrow$  boat  $\rightarrow$  half-chair  $\rightarrow$  chair. The half-chair form is not stable because the hydrogen atoms at the foot are eclipsed with those on the adjacent carbons, and because of this fact, there is some angular strain. These angular strains occur because the molecule is nearly planar and are destabilized by torsional strain. The half-chair conformation is about 40 kJ mol<sup>-1</sup> higher than that of the chair conformation. The boat conformation is also unstable because, although there is not angular strain, several of the C–H bonds are now eclipsed.

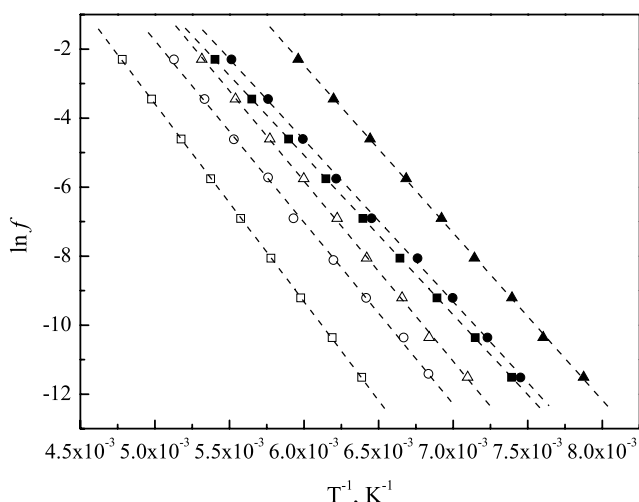


Fig. 5. Arrhenius plot of two  $\gamma$  processes corresponding to the three polymers under study. ( $\square$ ,  $\blacksquare$  P2MCHMA;  $\circ$ ,  $\bullet$  P3MCHMA;  $\triangle$ ,  $\blacktriangle$  P4MCHMA).

Table 2  
Summary of energy contributions (kJ mol<sup>-1</sup>), dipolar moments and geometric parameter (Å) derived from FF-optimized geometries, corresponding to chair–chair interconversion of *cis*- and *trans*-isomers of P2MCHMA, P3MCHMA and P4MCHMA

|  | Chair → boat → half chair → chair |       |       |       | Chair → half chair → boat → chair |       |       |       |
|--|-----------------------------------|-------|-------|-------|-----------------------------------|-------|-------|-------|
|  | <i>cis</i> -P2MCHMA               |       |       |       | <i>trans</i> -P2MCHMA             |       |       |       |
| SE                                       | -13.44                            | 17.64 | 39.47 | -4.62 | -13.02                            | 30.65 | 9.66  | -5.46 |
| μ  | 1.765                             | 1.758 | 1.795 | 1.760 | 1.758                             | 1.755 | 1.752 | 1.765 |
| <i>d</i> <sub>O-CH<sub>3</sub></sub> (Å) | 2.89                              | 2.89  | 2.92  | 2.85  | 3.76                              | 2.85  | 2.85  | 2.91  |
|  | <i>trans</i> -P3MCHMA             |       |       |       | <i>cis</i> -P3MCHMA               |       |       |       |
| SE                                       | -13.02                            | 11.76 | 36.11 | -5.04 | -12.18                            | 31.91 | 11.76 | -5.04 |
| μ  | 1.763                             | 1.750 | 1.75  | 1.755 | 1.754                             | 1.752 | 1.749 | 1.756 |
| <i>d</i> <sub>O-CH<sub>3</sub></sub> (Å) | 4.34                              | 4.54  | 4.49  | 4.45  | 4.92                              | 4.90  | 4.90  | 3.07  |
|  | <i>cis</i> -P4MCHMA               |       |       |       | <i>trans</i> -P4MCHMA             |       |       |       |
| SE                                       | -13.02                            | 10.08 | 35.27 | -5.04 | -12.18                            | 33.59 | 17.22 | -5.46 |
| μ  | 1.763                             | 1.749 | 1.76  | 1.754 | 1.754                             | 1.751 | 1.747 | 1.763 |
| <i>d</i> <sub>O-CH<sub>3</sub></sub> (Å) | 4.64                              | 5.68  | 5.59  | 4.78  | 5.72                              | 5.35  | 4.81  | 4.71  |

SE, strain energy; μ, dipole moment.

Moreover, van der Waals repulsions between the two hydrogens at the axial position of C1 and C4 are present. The boat conformation has a energy of about 20 kJ mol<sup>-1</sup> higher than that of the chair conformation.

When the cyclohexyl ring is bounded to the polymer chain, the motion is something different to that before mentioned. In this case, the motion, which produces the transition from one chair form to another fixes the oxycarbonyl group to the main chain and so this group remains more or less in the same position after the chair-to-chair transition. In the chair-to-chair transition, the bond linking the methyl group in the 4-position to the ring, retains its orientation in the space. However, this bond is turned in an angle of about 109° in polymers having the methyl group in the 2- or 3-position. As a result, the temperature of the relaxation peak associated to the chair-to-chair transition should be larger for the polymers with the methyl group in position 2- or 3 than for those having the methyl group in 4-position, in agreement with our results.

Molecular mechanics calculations have been carried out with the two, *cis*- and *trans*-isomers. Table 2 summarizes the energy terms and the significant bond lengths derive from the force field (MMX) optimized geometries of the one-unit model (monomer) compound for the three poly(methylcyclohexyl methacrylate)s studied in *cis* and *trans* conformations.

Our results show that the axial position of the methyl group in the cyclohexyl ring in all models studied is energetically less favorable than the equatorial position, and in the chair-to-chair transition the equatorial substituent becomes axial and vice versa (Table 2). The fact that the axial position of the methyl group was less favorable can be mainly due to the interaction between the methyl group and the hydrogen atoms also in axial position.

Table 3 summarizes the energy barrier and a scheme of how, chair-to-chair transition takes place in each conformer. The energy barrier was calculated as the difference between the energy of the less favorable conformation (the half-chair) and the more stable conformation (chair). According to our results, the *cis*-isomer will be more hindered in its transition than the *trans*-isomer in P2MCHMA and P4MCHMA. The inverse situation is present in the case of P3MCHMA.

Because to the fact that the motions of cyclohexyl ring require a larger volume when the methyl group is bounded to the cyclohexyl ring, an increase in activation energy of the γ-relaxations should be expected in the substituted polymers with respect to PCHMA. In fact, the energy barrier calculated for all polymers follows the tendency given by *cis*-P2MCHMA > *trans*-P3MCHMA > *cis*-P4MCHMA > *trans*-P4MCHMA > *cis*-P3MCHMA > *trans*-P2MCHMA > PCHMA. This sequence is in agreement with that obtained from the loss dielectric simulation (Table 1).

The higher and the smaller energy barrier correspond, respectively, to the *cis*- and *trans*-isomers of P2MCHMA. The difference between the energy barrier calculated for *cis*- and *trans*-isomers for each poly(methyl cyclohexyl methacrylate) follows the trend given by Δ*E*<sub>a</sub>(P2MCHMA) > Δ*E*<sub>a</sub>(-P3MCHMA) > Δ*E*<sub>a</sub>(P4MCHMA). Thus, when the distance between the methyl group of the cyclohexyl ring and the remainder part of the molecule is higher, the difference between the barrier energy of *cis*- and *trans*-isomers is small.

In order to give account of the different heights of the peaks for the *cis*- and *trans*-isomers, two possible explanations [1] has been proposes. A first explanation consider the blocking of the chair-to-chair transition due to steric hindrance by the surroundings. A second explanation should be possible on the basis of the difference of the conformational energy between the two isomers.

In order to adress this problem, the distances between the oxygen atom and the methyl group obtained by mechanical simulation for the three polymers, as have been summarized in Table 2. In the case of *trans*-P4MCHMA the methyl group in the equatorial position protrudes from the molecule in the equatorial position ( $\bar{d}_{\text{O-CH}_3}^{\text{eq}} \sim 5.7$  Å) more than in the axial position ( $\bar{d}_{\text{O-CH}_3}^{\text{ax}} \sim 4.7$  Å), whereas for the *cis*-P4MCHMA  $\bar{d}_{\text{O-CH}_3}^{\text{eq}} \sim \bar{d}_{\text{O-CH}_3}^{\text{ax}} \sim 4.7$  Å. In the case of P3MCHMA, the *cis*-isomer has  $\bar{d}_{\text{O-CH}_3}^{\text{eq}} \sim 4.9$  Å,  $\bar{d}_{\text{O-CH}_3}^{\text{ax}} \sim 3.7$  Å whereas for the *trans*-isomer,  $\bar{d}_{\text{O-CH}_3}^{\text{eq}} \sim \bar{d}_{\text{O-CH}_3}^{\text{ax}} \sim 4.4$  Å. However, in this case the differences observed are lesser than in the previous case. Finally, for P2MCHMA, one has, respectively for the *trans*- and *cis*-isomers  $\bar{d}_{\text{O-CH}_3}^{\text{eq}} \sim 3.8$  Å,  $\bar{d}_{\text{O-CH}_3}^{\text{ax}} \sim 2.9$  Å,  $\bar{d}_{\text{O-CH}_3}^{\text{eq}} \sim \bar{d}_{\text{O-CH}_3}^{\text{ax}} \sim 2.9$  Å). The average distance shows the

Table 3  
Energy barrier ( $\text{kJ mol}^{-1}$ ) calculated by MMX for the chair–chair interconversion

|                       |       |       |       |       | Energy barrier<br>( $\text{kJ mol}^{-1}$ ) |
|-----------------------|-------|-------|-------|-------|--|
|                       |       |       |       |       |  |
| PCHMA                 | 41.68 | 64.19 | 84.71 | 42.18 | 43.03                                      |
| <i>cis</i> -P2MCHMA   | 42.54 | 73.58 | 95.17 | 51.29 | 52.63                                      |
| <i>trans</i> -P3MCHMA | 42.82 | 67.54 | 91.74 | 50.76 | 48.92                                      |
| <i>cis</i> -P4MCHMA   | 42.62 | 65.85 | 90.98 | 50.86 | 48.36                                      |
|                       |       |       |       |       |  |
| <i>trans</i> -P2MCHMA | 42.95 | 86.41 | 65.51 | 50.15 | 43.46                                      |
| <i>cis</i> -P3MCHMA   | 43.44 | 87.72 | 67.66 | 50.55 | 44.27                                      |
| <i>trans</i> -P4MCHMA | 43.57 | 89.39 | 72.87 | 50.40 | 45.82                                      |

following trend,  $\bar{d}_{\text{O-CH}_3}(\text{P4MCHMA}) > \bar{d}_{\text{O-CH}_3}(\text{P3MCHMA}) > \bar{d}_{\text{O-CH}_3}(\text{P2MCHMA})$ . Thus, when this distance is higher, the methyl group protrudes more from the molecule and being more hindered the chair-to-chair transition. The height of the maximum should be lower, as can be shown in the experimental results obtained from the DRS [16] and TSDC (inset Fig. 1) measurements.

According to the distance analyzed,  $\bar{d}_{\text{O-CH}_3}$ , the height of the peak of the *cis*-isomer should be higher than that corresponding to the *trans*-isomer, for the P2MCHMA and P4MCHMA, and the height of the peak of the *cis*-isomer should be smaller than that corresponding to the *cis*-isomer for the P3MCHMA. At this respect, the values of  $\epsilon''_{\text{max}}^{(i)}$  obtained in the fitting procedure of loss permittivity spectra to the empirical FK equation, allow us to make a comparison between the heights of the peaks of *cis*- and *trans*-isomers. These results show that the peak for *cis*-P4MCHMA is higher than that for *trans*-P4MCHMA, in agreement with the calculated distance between the oxygen atom and the methyl group. However, the contrary situation is observed in the case of P2MCHMA and P3MCHMA.

In order to interpret these results, we analyze the strain energy (SE) values, defined as the difference between the steric energy of the molecule and the steric energy if all the components of the molecule were in a strain free environment. For poly(methyl cyclohexyl methacrylate)s we observe high values for SE in half-chair conformations (Table 2). Moreover, in P2MCHMA and P4MCHMA,  $\text{SE}(\text{cis-conformation}) > \text{SE}(\text{trans-conformation})$  and for P3MCHMA  $\text{SE}(\text{trans-conformation}) > \text{SE}(\text{cis-conformation})$ . The difference between *cis*-SE and *trans*-SE,  $\Delta\text{SE}$ , for the polymers, follows the sequence P2MCHMA(8.8) > P3MCHMA(4.2) > P4MCHMA(1.6).

Thus, in the case of P2MCHMA, the value of the SE makes the *cis*-conformation of intermediate half-chair, less stable by  $8.8 \text{ kJ mol}^{-1}$ , than the *trans*-conformation and in the case of P3MCHMA, the value of the SE makes the *trans*-conformation of intermediate half-chair, less stable by  $4.2 \text{ kJ mol}^{-1}$ , than the *cis*-conformation. For this reason one should expect higher peaks for *trans*-isomers in P2MCHMA and *cis*-isomer in P3MCHMA. Thus although a smaller peak should be expected when the larger the molecular environment is present, the height of the *cis*-peaks in P2MCHMA and of the *trans*-peaks in P3MCHMA, are mainly controlled by the SE. In these polymers, only a small fractions of the *cis*-rings (P2MCHMA) and of the *trans*-rings (P3MCHMA) are able, due to the high values of SE, to take place in the motion provoking the *cis*-relaxation (P2MCHMA) and the *trans*-relaxation (P3MCHMA).

#### 4. Conclusions

Methacrylic polymers like P2MCHMA, P3MCHMA and P4MCHMA show complex TSDC spectra. In fact at least four relaxations zones labeled  $\alpha$ ,  $\beta$ ,  $\gamma$  and  $\delta$  in decreasing order of temperature are observed.

A combination of DRS, TSDC and molecular mechanics calculations allow us to obtain more conclusive results on the fine structure of the  $\gamma$ -relaxation zone. It is concluded that two  $\gamma$ -relaxation processes probably due to *cis*- and *trans*-conformers are present in all the polymers under study. The presence of two peaks is more clearly visualized in TSDC spectra than in conventional DRS. However, DRS measurements show that the height of this peak is lower for

the methyl-substituted cyclohexyl rings (P2MCHMA, P3MCHMA, and P4MCHMA) than for the unsubstituted (PCHMA). This is in agreement with the assumption that the cyclohexyl ring is the responsible of the process associated at this peak, because the height of this peak is related to the proportion of cyclohexyl groups in the molecule. The apparent activation energies for the  $\gamma$  peaks according to TSDC measurements are close to the values derived from our empirical force field molecular mechanics calculations. We have observed the same tendency in both type of analysis. According with this result we can conclude than the principal responsible of these relaxation peaks are the chair-to-chair interconversion. Although, molecular dynamic calculations carried out for other related polymers, show than the dielectric  $\gamma$ -relaxations cannot be exclusively attributed to simple chair-to-chair conformational transitions in the cyclohexyl ring [1,5]. Molecular motions associated to the side groups, such as conformational transitions through O–C $\gamma$  and CH–C\*O\* bond, are probably also involved in the complex  $\gamma$  subglass absorption observed in this type of polymers.

A possible explanation of the relative height peaks associated to the cis- and trans-conformers of P2MCHMA and P3MCHMA is given in terms of the values of the strain energy (SE).

### Acknowledgements

G.D., MJSS and RDC gratefully acknowledge to CICYT for grant MAT2002-04042-C02-01. L.G. and D.R. acknowledge to FONDECYT Grant 1010726 for financial help. C.P thanks to CONICYT and DIPUC for a Doctoral fellowship. Partial financial support from MECESUP through projects PUC 0004 and MECESUP-REDES UCH O116 is also acknowledged.

### References

- [1] (a) Heijboer J. Molecular basis of transitions and relaxation. In: Meier DJ, editor. Midland macromolecular monographs, vol. 4. Breach: Gordon; 1978. p. 297.  
(b) Heijboer J. PhD Thesis, Leiden, the Netherlands; 1972
- [2] Karpovich JJ. Chem Phys 1954;22(10):1767–73.
- [3] Saiz E, Riande EJ. Chem Phys 1995;103(9):3832–8.
- [4] Kotlik P, Heidingsfeld V, Zelinger JJ. Polym Sci, Part A: Polym Chem 1975;13(6):1417–25.
- [5] Díaz-Calleja R, Saiz E, Riande E, Gargallo L, Radić D. J Polym Sci, Polym Phys 1994;32(6):1069–77.
- [6] Díaz-Calleja R, Sanchis MJ, Aravena M, Riande E, Guzmán. J Macromol Symp 2003;191:177–90.
- [7] Burtle JG, Turek WNJ. Org Chem 1954;19(10):1567–70.
- [8] Gargallo L, Méndez I, Radić D. Makromol Chem 1983;184(5):1053–60.
- [9] van Turnhout J. Thermally stimulated discharge of polymer electretes. Amsterdam: Elsevier; 1975.
- [10] (a) Phillip T, Cook RL, Malloy TB, Allinger NL, Chang S, Yuh Y. J Am Chem Soc 1981;103(9):2151–6.  
(b) Allinger NL, Yuh H. Quantum Chem Prog Exchange QCPE 1981;13:395.
- [11] Allinger NL, Zhou X, Bergsma. J Mol Struct (Theochem) 1994;118(1):69–83.
- [12] Burkert U, Allinger NL. Mol Mech ACS Monogr Ser Number 1982;177.
- [13] Available from Serena Software, PO Box 3076 Bloomington IN 47402-3076.
- [14] Allinger NL, Sprague JT. J Am Chem Soc 1973;95(12):3893–907.
- [15] Press WH, Teukolsy SA, Vetterling WT, Flannery BP. Numerical recipes in C. 2nd ed. New York: Cambridge University Press; 1992.
- [16] Domínguez-Espinosa G, Sanchis MJ, Díaz-Calleja R, Pagueyuy C, Gargallo L, Radić, D. Polymer 2005;46:8028–33.
- [17] Vanderschueren J, Gasiot J. In: Bräunlich P, editor. Thermal stimulated relaxation in solids. Berlin: Springer; 1979.
- [18] Lacabane C, Chatain D. J Polym Sci B, Polym Phys 1976;11:2315.
- [19] Bucci C, Fieschi R, Guidi G. Phys Rev 1966;148(2):816–20.
- [20] Zielinski M, Kryszewski M. Phys Status Solidi A 1977;42(1):305–14.
- [21] Shimizu H, Nakayama K. J Appl Phys 1993;74(3):1597–605.
- [22] Perlman MM, Unger S. J Appl Phys 1974;45(6):2389–93.
- [23] Fuoss R, Kirkwood JE. J Am Chem Soc 1941;63:385–9.